Topographical attributes to predict soil hydraulic properties along a hillslope transect

Feike J. Leij,[1] Nunzio Romano,[2] Mario Palladino,[2] Marcel G. Schaap,[1] and Antonio Coppola[3]

Received 6 August 2002; revised 10 October 2003; accepted 6 November 2003; published 27 February 2004.

[1] Basic soil properties have long been used to predict unsaturated soil hydraulic properties with pedotransfer function (PTFs). Implementation of such PTFs is usually not feasible for catchment-scale studies because of the experimental effort that would be required. On the other hand, topographical attributes are often readily available. This study therefore examines how well PTFs perform that use both basic soil properties and topographical attributes for a hillslope in Basilicata, Italy. Basic soil properties and hydraulic data were determined on soil samples taken at 50-m intervals along a 5-km hillslope transect. Topographical attributes were determined from a digital elevation model. Spearman coefficients showed that elevation (z) was positively correlated with organic carbon (OC) and silt contents (0.62 and 0.59, respectively) and negatively with bulk density (ρ_b) and sand fraction (-0.34 and -0.37). Retention parameters were somewhat correlated with topographical attributes z, slope (β), aspect ($\cos\phi$), and potential solar radiation. Water contents were correlated most strongly with elevation (coefficient between 0.38 and 0.48) and aspect during "wet" conditions. Artificial neural networks (ANNs) were developed for 21 different sets of predictors to estimate retention parameters, saturated hydraulic conductivity (K_s), and water contents at capillary heads h = 50 cm and 12 bar (10^3 cm). The prediction of retention parameters could be improved with 10% by including topography (RMSE = 0.0327 cm^3 cm^{-3}) using textural fractions, ρ_b, OC, z, and β as predictors. Furthermore, OC became a better predictor when the PTF also used z as predictor. The water content at h = 50 cm could be predicted 26% more accurately (RMSE = 0.0231 cm^{3}cm^{-3}) using texture, ρ_b, OC, z, β, and potential solar radiation as input. Predictions of ANNs with and without topographical attributes were most accurate in the wet range ($0 < h <$ 250 cm). Semivariograms of the hydraulic parameters and their residuals showed that the ANNs could explain part of the (spatial) variability. The results of this study confirm the utility of topographical attributes such as z, β, $\cos\phi$, and potential solar radiation as predictors for PTFs when basic soil properties are available. A next step would be the use of topographical attributes when no or limited other predictors are available. *INDEX TERMS:* 1824 Hydrology: Geomorphology (1625); 1866 Hydrology: Soil moisture; 1875 Hydrology: Unsaturated zone; *KEYWORDS:* hydraulic conductivity, neural networks, pedotransfer function, soil, terrain analysis, water retention

Citation: Leij, F. J., N. Romano, M. Palladino, M. G. Schaap, and A. Coppola (2004), Topographical attributes to predict soil hydraulic properties along a hillslope transect, *Water Resour. Res.*, *40*, W02407, doi:10.1029/2002WR001641.

1. Introduction

[2] Quantifying flow and transport processes in the vadose zone is plagued by the well-known difficulty to estimate the hydraulic properties. Pedotransfer functions (PTFs) may be employed to predict these properties, viz. the soil water retention, $\theta(h)$, and hydraulic conductivity, $K(\theta)$ or $K(h)$, functions where θ is the volumetric soil water content, h is the soil capillary pressure head, and K is the hydraulic conductivity. PTFs have been proposed to conveniently predict unsaturated soil hydraulic properties from pedological predictors [*Rawls et al.*, 1982; *Bouma*, 1989]. The convenience pertains to the avoidance of hydraulic measurements by relying on data already available or more easily measured. However, a fairly comprehensive set of predictor and hydraulic data is required to establish the PTFs. Furthermore, this is an empirical approach and PTFs should not be used to predict hydraulic data outside the range of conditions for which they have been calibrated while the uncertainty of the predictions needs to be quantified [*Schaap and Leij*, 1998]. Basic soil properties such as textural fractions, bulk density and organic matter content have been widely used as predictors [*Minasny et al.*, 1999; *Schaap et al.*, 2001; *Wösten et al.*, 2001].

[1] George E. Brown Jr. Salinity Laboratory, Agricultural Research Service, USDA and Department of Environmental Sciences, University of California, Riverside, California, USA.
[2] Department of Agricultural Engineering, University of Naples, Naples, Italy.
[3] Dipartimento Tecnico Economico per la Gestione del Territorio Agricolo-forestale, University of Basilicata, Potenza, Italy.

0043-1397/04/2002WR001641

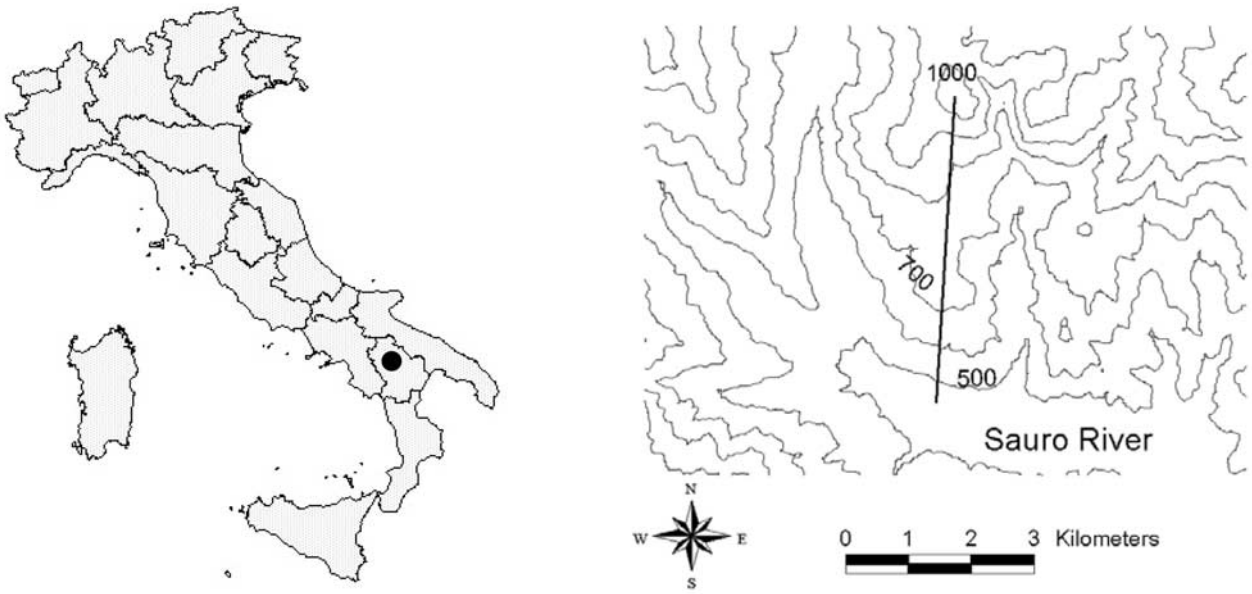

Figure 1. Location and topography of study site.

[3] At the catchment scale, where even adequate measurement of basic soil properties may not be feasible, the question arises if topographical attributes could be used to replace or augment basic soil properties as predictors in PTFs. Soil formation is affected by vegetation, parent material, microclimate, moisture regime, and material transport; all of which are influenced by topography. This (indirect) influence of topography on soil properties and processes has long been recognized [*Ruhe*, 1956; *Walker et al.*, 1968; *Carter and Ciolkosz*, 1991]. Topographical attributes may therefore be correlated with hydraulic properties. Soil attributes will convey some of the correlation more directly, but it is also possible that topographical attributes contain new information for the prediction. Topographical attributes are widely available with the advent of digital elevation models (DEMs) and digital terrain analysis techniques. The added resolution provided by topographical attributes may help to better interpret and predict flow and transport in complex natural soil systems.

[4] The catchment area of the Sauro river, which is located in the Basilicata region of southern Italy (Figure 1), was selected as a case study for quantifying and elucidating the hydrology at the basin scale as well as surface erosion and land degradation. Soil, landscape and hydraulic properties were investigated in order to predict and explain local-scale runoff and infiltration. These processes can, in turn, be used to model integrated catchment behavior through upscaling. Undisturbed soil samples were collected along a hillslope transect in the study area to determine basic soil properties, water retention, and hydraulic conductivity. Furthermore, a landscape analysis was conducted based on aerial photography, topographic and geological maps, and a field survey was carried out to delineate soil units with different hydraulic properties [*Santini et al.*, 1999].

[5] The study site is located in a hilly area with a dynamic geomorphology and a climate with long periods of drought and some intense rainfall during fall and winter months. These conditions are prevalent around the Mediterranean and have resulted in soils with distinct characteristics [*Yaalon*, 1997]. Many soils are formed on calcareous parent material (i.e., limestone, carbonate-cemented sandstone, calcareous clayey sediments) and the seasonal rainfall promotes leaching and deep precipitation of carbonates and in some cases illuviation of clay material. The topography and the strong seasonality of the rainfall pose particular challenges for efficient and sustainable agricultural production and water management. In order to attain such a scenario of sustainability, it is imperative to understand the role of hydrology at the catchment scale where different polypedons occur. *Romano and Santini* [1997] applied PTFs by *Gupta and Larson* [1979], *Rawls et al.* [1982], *Rawls and Brakensiek* [1989] and *Vereecken et al.* [1989], all of which exclusively use basic soil data as input, to predict water contents at capillary pressure heads h = 10, 100, and 1000 cm along the transect. The predicted water contents were normally distributed and the PTFs appeared to preserve the spatial structure of the observed water content.

[6] For the selected hillslope, topographical attributes could be especially useful as predictors because changes in geological conditions and other soil formation factors are more pronounced. The present work involves the use of topographical attributes to predict hydraulic properties at sites where soil attributes were also available. Of course, an important application is the use of topographical attributes ''to fill gaps'' when no or limited soil attributes are available. Most if not all conceptually based watershed models require data for a large number of locations where no soil or hydraulic properties will be available. Topographical data could then be used to infer soil properties or directly estimate hydraulic properties. The different types of interpolation strategies are further discussed by *Sinowsky et al.* [1997] and *Heuvelink and Pebesma* [1999]. Interpolation between points where soil properties have been sampled

should account for topography because of the impact that organized patterns will have on model response [*Merz and Plate*, 1997; *Western et al.*, 2001].

[7] Models for the land surface have long been employed by geomorphologists [*Ruhe*, 1975]. More recently, several studies have appeared that investigated correlation with soil water content [*Famiglietti et al.*, 1998; *Western et al.*, 1999] or retention data [*Pachepsky et al.*, 2001]. *Famiglietti et al.* [1998] and *Western et al.* [1999] monitored surface water content over time by destructive sampling and by time domain reflectometry, respectively. The water content of the root zone is most important in energy balance and has a profound effect on heat and mass exchange at the earth-atmosphere boundary. Only the surface water content (i.e., up to 5-cm depth) can be measured remotely for low vegetation sites. Surface water content is not an intrinsic variable; it depends on factors such as precipitation, solar radiation, vegetation, depth of water table, and antecedent moisture regime and it is subject to considerable temporal variability. Correlations between topographical attributes and soil hydraulic functions would be of greater interest for the modeling of (sub)surface flow.

[8] Elevation may affect soil hydraulic properties because soil formation factors such as parent material, temperature and vegetation change with altitude. The structural and textural properties of surface soils, and hence their hydraulic properties, will change with elevation. Most studies have reported that water contents tend to be lower at higher elevations [e.g., *Hawley et al.*, 1983]. The maximum slope (angle) of the soil surface determines the gradient for the flow of water and any dissolved matter on the surface and even near the surface. Areas with steeper slopes will experience less infiltration and crust formation and more surface runoff; the surface water content is likely to be lower [*Moore et al.*, 1988] and the hydraulic conductivity higher [*Casanova et al.*, 2000]. *Pachepsky et al.* [2001] reported a decrease in water retention for steeper slopes at intermediate capillary heads (r^2 of 0.451 and 0.345 at h = 100 and 330 cm, respectively). Aspect or slope orientation characterizes the direction of the slope and hence the flow; it is used to establish contributing areas. *Hanna et al.* [1982] observed higher available water contents and *Cerdà* [1997] reported higher infiltration rates for north-facing slopes in the northern hemisphere. In Chile, *Casanova et al.* [2000] found a higher conductivity for a south facing slope. Higher organic matter and clay contents for the south-facing slope presumably lead to more stable macropores and a higher conductivity. Aspect and slope both affect the intensity of rain and radiation input, which will have repercussions for soil attributes and hydraulic properties.

[9] Land surface curvature is an important determinant of lateral flow patterns; depressed areas will be wetter than elevated or planar areas with corresponding differences in sedimentation patterns and biological activity. Profile or slope curvature is quantified by changes in slope angle along the aspect, negative values indicate a concave streamline with decelerating flow while positive values are found for convex surfaces with accelerating flow. Tangential curvature quantifies curvature in the plane transversal to aspect, this variable conveys information on convergence and divergence of lateral flows. If the curvature is measured in the horizontal plane, i.e., pertaining to contours, it is referred to as plan curvature. The value for the mean curvature enumerates the overall concavity or convexity of the surface. *Famiglietti et al.* [1998] showed a negative correlation between surface water content and three types of curvature. *Pachepsky et al.* [2001] found that water content at h = 100 and 330 cm were negatively correlated with profile curvature, i.e., accelerating flow lowers retention (with r^2 of 0.266 and 0.310, respectively) and positively correlated with tangential curvature, i.e., divergence promotes retention (with r^2 of 0.423 and 0.432, respectively). Potential solar radiation, which is determined from the slope, aspect and solar position, affects evapotranspiration; the water content will be lower for surfaces receiving more solar radiation [*Western et al.*, 1999]. A correlation between solar radiation and hydraulic properties is conceivable because soil formation is affected by moisture regime, temperature and vegetation. Contributing area and slope determine the flux and gradient for overland flow. The wetness index, which is useful to estimate surface runoff and erosion, has been shown to be positively related with surface water content [*Moore et al.*, 1988; *Famiglietti et al.*, 1998; *Western et al.*, 1999]. Other topographical attributes, such as the compound stream power and sediment transport capacity indices [*Moore et al.*, 1993] and the elevation-relief ratio for skewness of elevation [*U.S. Army Corps of Engineers*, 1993], have also been used in soil classification and erosion studies.

[10] It appears plausible that topographical attributes can improve PTFs. However, *Famiglietti et al.* [1998] cite several studies where there was no significant correlation between topographical attributes and soil water content. If there is significant correlation with hydraulic properties, it will be considerably less than for soil attributes [*Pachepsky et al.*, 2001]. Furthermore, use of topographical attributes that are marginally correlated with hydraulic properties could lead to poorer performance of PTFs due to overparameterization.

[11] The uncertainty associated with topographical predictors also hinges on the spatial resolution and variability of topographical data. *Western et al.* [1999] did investigate how well water content, also subject to temporal variability, was predicted by terrain attributes over different scales. The potential radiation index explains little of the variance while the wetness index explains some of the spatial variance, particularly at larger lag distances (>150 m). Of course, not all of the spatial variability is topographically organized and only the organized part can be explained by terrain attributes. Variogram data indicated that more than half of the unexplained variance occurs at a scale less than the 10-m grid of the DEM. *Western et al.* [1999] postulated that variability between the DEM and hillslope scales occurs due to routed lateral flow, which may be explained by wetness index and upslope area. Variability at the hillslope and catchment scales could be explained by aspect and soils or vegetation, respectively.

[12] In view of the above, this study was intended to detect correlations between hydraulic data and topographical attributes and to make use of them in PTFs. More detailed observations will be needed to elucidate the mechanisms by which topography determines the magnitude of hydraulic properties. The specific objectives are as follows:

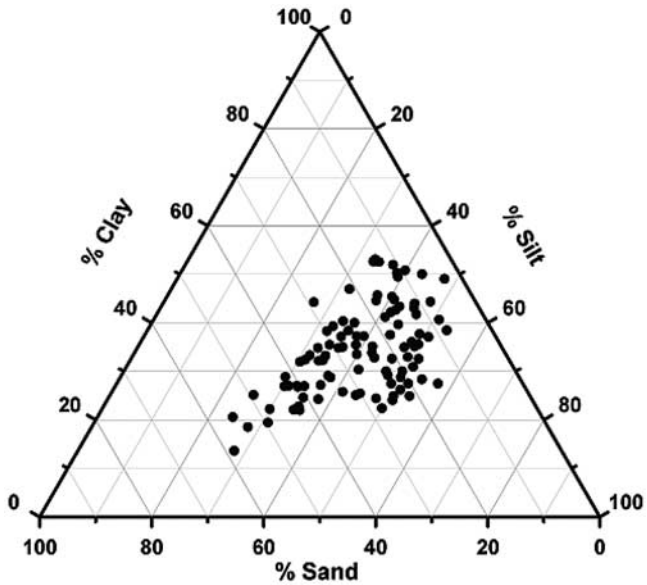

Figure 2. Textural distribution of samples.

(1) investigate correlations between soil and topographical attributes, retention data, and hydraulic parameters for a hillslope in Basilicata, Italy, (2) calibrate PTFs with soil and/or topographical attributes as predictor using neural network analysis, and (3) examine if topographical attributes can improve PTFs by considering different soil moisture regimes and variability of residuals.

2. Materials and Methods

2.1. Site

[13] The data that are analyzed in this study were collected from a hillslope in the Sauro River catchment area near the village of Guardia Perticara in Basilicata, Italy. The soils in the Sauro valley are typical for those found in the Mediterranean with a xeric moisture and mesic thermic regime. Soil type ranges from Vertisols to Mollisols and the soil genesis is greatly affected by the dynamic geomorphology of the region with slides, slide terraces and accumulation glacis with changing slopes and aspects [*Santini et al.*, 1999]. In many parts of the catchment the slope is too steep for the development of mature soils and the surface horizon tends to be thin. The vegetation consists of deciduous/perennial trees and shrubs, the latter are partly present on land that was used for cattle grazing and horticulture prior to 1955.

[14] One hundred soil samples were taken at 50-m intervals along a 5-km transect that runs in the same NE/SW direction as the hillslope. Figure 1 shows a contour map with elevations as well as the transect along which samples were taken. The actual sampling positions were determined with GPS. The transect is located at the boundary of different catchment areas. The first sample was taken at an elevation of 1072 m whereas the last sample was taken 472 m above sea level near the Sauro river. Undisturbed samples were taken between a 5- to 12-cm depth using 7-cm long steel cylinders with an inner diameter of 7.2 cm to determine water retention and saturated hydraulic conductivity in the laboratory [*Romano and Santini*, 1997]. An additional disturbed sample was taken from the hole created by the undisturbed sampling.

2.2. Soil Attributes and Hydraulic Properties

[15] Several "basic" soil properties were determined according to standard methodology [*Dane and Topp*, 2002]. The dry bulk density (ρ_b) was obtained from the weight of a volumetric sample after oven drying at 105°C. Particle density (ρ_s) was measured with the pycnometer method and total porosity was estimated according to the relation $\varepsilon = 1 - \rho_b/\rho_s$. The mass fraction of organic carbon (OC) was determined with the dichromate method. Finally, the percentages clay (<2 μm), silt (2–50 μm), and sand (50–2000 μm) were established with the hydrometer method and sieving. Figure 2 shows the textural distribution of the samples. The soil tends to be fine-textured with a relatively large silt fraction, presumably of aeolian origin.

[16] Prior to the hydraulic measurements, the 7-cm long "undisturbed" samples were placed on a cloth-covered perforated Perspex disk and gradually saturated from the bottom using a 0.01 *M* $CaCl_2$ + 0.2 g/L thymol solution made up of de-aired water. For the water retention, water content was measured gravimetrically at successively higher soil capillary heads with average values of 10, 20, 50, 90, and 150 cm water using a suction table apparatus [*Romano et al.*, 2002]. For the water content at saturation, a fictitious value of 0.1 cm was assumed for h to allow plotting on a logarithmic scale. A membrane plate apparatus was used to determine retention at heads of 3, 6 and 12 bar (10^3 cm). The saturated hydraulic conductivity, K_s, was determined according to the falling head method.

[17] The retention data were parameterized with the equation by *van Genuchten* [1980]:

$$\frac{\theta - \theta_r}{\theta_s - \theta_r} = [1 + (\alpha h)^n]^{-(1-1/n)} \quad (1)$$

where h is the capillary pressure head (cm), θ_r and θ_s are the residual and saturated water contents (cm^3cm^{-3}), and α (cm^{-1}) and n are parameters that determine the shape of the retention curve. The value for α is inversely related to the "air entry" value with coarse-textured soils having a higher α. Soils with abrupt changes of the slope of the $\theta(h)$ curve, i.e., well-sorted or coarse-textured soils, tend to have high values for n. The "vG" parameter set $\{\theta_r, \theta_s, \alpha, n\}$ was optimized using the Simplex routine or Amoeba algorithm [*Press et al.*, 1988].

2.3. Topographical Attributes

[18] The topography of the study site was characterized with a 30 × 30-m grid size Digital Elevation Model from contour maps developed in ArcView using interpolation between 25-m isolines. Topographical variables were obtained from this DEM with the GRASS (Geographic Resources Analysis Support System) software for geographic information systems [*U.S. Army Corps of Engineers*, 1993]. The algebraic expressions to compute these variables are obtained from a scheme involving a moving 3 × 3 elevation kernel centered around the location of interest [*Mitášová and Hofierka*, 1993; *Moore et al.*, 1993]. The surface is described as a bivariate function according to $z = f(x, y)$ where z denotes vertical position and x and y are horizontal positions along the west-east and south-north directions,

respectively. First- and second-order derivatives f_x, f_y, f_{xx}, f_{yy}, and f_{xy} were obtained by finite differencing. Following *Moore et al.* [1993], the following auxiliary variables are defined:

$$p = f_x^2 + f_y^2 \quad , \quad q = p + 1 \tag{2}$$

The maximum slope, β (degrees), aspect, ϕ (degrees clockwise from north), profile (*PC*) and tangential (*TC*) curvature (1/m) are computed according to [*U.S. Army Corps of Engineers*, 1993]:

$$\beta = \arctan\left(\sqrt{p}\right) \tag{3}$$

$$\phi = 180 - \arctan\left(f_y/f_x\right) + 90\left(f_x/|f_x|\right) \tag{4}$$

$$PC = \frac{f_{xx}f_x^2 + 2f_{xy}f_xf_y + f_{yy}f_y^2}{pq^{3/2}} \tag{5}$$

$$TC = \frac{f_{xx}f_y^2 - 2f_{xy}f_xf_y + f_{yy}f_x^2}{pq^{1/2}} \tag{6}$$

Additional topographical attributes that were used are the mean curvature, *MC* (the arithmetic mean of *PC* and *TC*) as well as (potential) solar radiation for the spring (21 March), *SpR*, summer (21 June), *SuR*, and winter (21 December), Note that solar radiation for the fall is equivalent to that for the spring. Topographical variables at the actual sample locations were interpolated with the nearest neighbor procedure using Surfer® version 7.00 (Golden Software, Inc., Golden, CO).

2.4. Preliminary Analysis

[19] Scatter diagrams were prepared to illustrate the behavior of hydraulic parameters versus potential predictors. Spearman rank-order coefficients were subsequently determined for correlation between all possible data pairs. The data consist of: soil attributes $\{\rho_b, \rho_s, \varepsilon$, OC, clay, silt, sand$\}$, topographical attributes $\{z, \beta, \cos\phi$, *PC*, *TC*, *MC*, *SpR*, *SuR*, and *WR*$\}$, hydraulic parameters $\{\theta_r, \theta_s, \alpha, n, K_s\}$, and retention data $\{\theta_{0.1}, \theta_{10}, \theta_{50}, \theta_{90}, \theta_{150}, \theta_{250}, \theta_{3b}, \theta_{6b}$, and $\theta_{12b}\}$.

2.5. Neural Network Analysis

[20] Artificial neural networks (ANNs) were developed to predict hydraulic parameters $\{\theta_r, \theta_s, \alpha, n, K_s\}$ and retention data $\{\theta_{50}, \theta_{12b}\}$ from different sets of predictors, partly selected based on Spearman ranking. Input parameters were scaled and α, n, and K_s were also log-transformed to obtain a more normal distribution. The ANNs consist of feed-forward back propagation networks with one hidden layer containing six hidden nodes and sigmoidal transfer functions. Optimization of the weights in the ANNs was performed by minimizing the squared residuals of the hydraulic parameters using the Levenberg-Marquardt algorithm. The networks were implemented with the TRAINLM routine of the neural network toolbox [*Demuth and Beale*, 1992] of MATLAB® version 4.0 (MathWorks Inc., Natick, MA). The bootstrap method was employed for randomized sampling with replacement to divide the 100-sample set in calibration and validation parts. The calibration and bootstrap procedure was repeated thirty times for each ANN. Further details are given by *Schaap and Leij* [1998].

[21] Predictions of the ANNs were assessed with the correlation coefficient, r, between measured and estimated values, the root mean square of errors (RMSE) and the mean error (ME):

$$\mathrm{RMSE} = \left[\frac{1}{N}\sum_{i=1}^{N}\left(\hat{f}_i - f_i\right)^2\right]^{1/2} \tag{7}$$

$$\mathrm{ME} = \frac{1}{N}\sum_{i=1}^{N}\left(\hat{f}_i - f_i\right) \tag{8}$$

where f denotes a water content for a particular capillary pressure head – either measured or computed according to equation (1) from optimized hydraulic parameters – or log K_s, $\hat{f}$ indicates the corresponding value as estimated with the ANN, and N is the number of data points.

[22] The following prediction efficiency, also known as the Nash-Sutcliffe index, was used to examine how well water retention could be predicted as a function of capillary pressure head with different ANNs:

$$\mathrm{PE}(h) = 1 - \frac{\sum_{i=1}^{N}\left[\theta(h)_{VG,i} - \theta(h)_{ANN,i}\right]^2}{\sum_{i=1}^{N}\left[\theta(h)_{VG,i} - \overline{\theta}(h)_{VG}\right]^2} \tag{9}$$

where N is again the number of samples (locations in this case), $\theta(h)_{VG,i}$ indicates the water content at a location as predicted with optimized vG parameters with $\overline{\theta}(h)_{VG}$ as the arithmetic mean for all positions at a particular h, and $\theta(h)_{ANN,i}$ is the water content predicted with the ANN for a location. Values of PE near unity indicate a very good prediction whereas negative values imply that merely using the mean of all observations would be better than using the ANN.

[23] Finally, semivariograms and periodograms were computed for observed variables and residuals. The semivariograms may be used to assess how well the ANNs explain variability in the spatial domain [*Goovaerts*, 1997] while periodograms serve a similar role for the spectral domain [*Shumway and Stoffer*, 2000].

3. Results and Discussion

3.1. Preliminary Analysis

[24] Figure 3 shows 35 scatter diagrams for qualitative assessment of correlation between predictors, i.e., ρ_b, OC, clay, silt, sand, z, and β, and hydraulic parameters. No correlation is apparent for θ_r. As far as θ_s is concerned, a strong negative correlation exists with bulk density and to a lesser extent with sand, there appears to be a positive correlation with organic carbon, silt, and also elevation. The parameter α is somewhat correlated with sand while a negative correlation may exist with clay, silt, elevation and slope. The dependency of n is less pronounced; there may

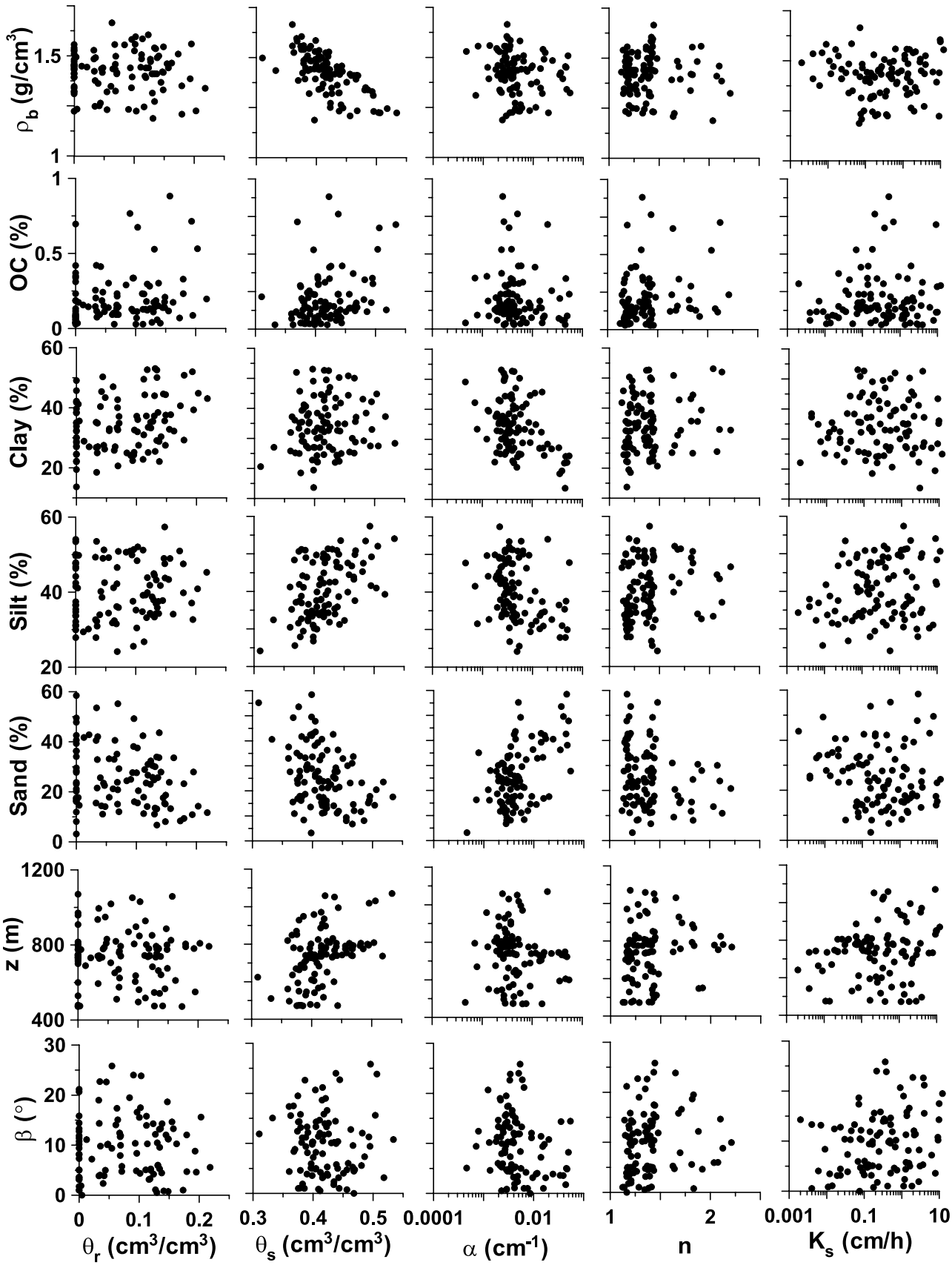

Figure 3. Scattergrams of θ_r, θ_s, α, n, and K_s as a function of ρ_b, organic carbon content, percentages clay, silt, and sand, elevation, and slope.

be a slight negative correlation with sand and a positive correlation with slope. No correlations are evident for K_s.

[25] Figure 4 shows the Spearman rank coefficients for correlation between pairs of different data types. Furthermore, the mean, standard deviation and units of all parameters are shown at the top and bottom of Figure 4. Most basic soil properties appear to be significantly correlated with most water contents but less so for the higher suctions ($h \geq 3$ bar), clay content being the exception. This may be because retention is determined using the pressure outflow procedure and because most basic soil properties are not as pertinent for water retention at higher suctions [*Schaap et al.*, 2001]. Among the hydraulic parameters, θ_s exhibits correlation with virtually all of the basic soil properties; α and, to a lesser extent, n are significantly correlated with about half of the properties, and θ_r is only influenced by sand and clay percentages. This is in line with previous findings [*Schaap et al.*, 2001]. No correlation was found between K_s and basic soil properties, which was already evident from the scatter diagrams. This lack of correlation is at odds with published PTFs for K_s [e.g., *Cosby et al.*, 1984; *Ahuja et al.*, 1989] but may be a result of sampling near the surface where K_s will be affected most by disturbances and biological activity.

[26] As far as topographical variables are concerned, these appear to be less correlated with hydraulic data than the basic soil properties. First, the correlation among topographical variables themselves. There was some correlation between elevation and slope (see Figure 1), but slope was more strongly correlated with potential radiation as it is used to compute the latter. Aspect exhibits some slight correlation with curvatures and, strongly, with spring and winter radiation but not with summer radiation due to the latitude of the site.

[27] Second, the correlation between water contents and topography. Elevation is correlated with water contents in the "wet" range ($h \leq 250$ cm) in a similar manner as silt, OC, and particle density. These soil attributes also exhibit correlation with elevation. Slope has a slight negative correlation for higher h, which is not present for slope-correlated soil attributes (OC and silt) and may be due to the lower clay content of soils with steeper slopes. Note that *Pachepsky et al.* [2001] also reported a somewhat negative correlation but for lower capillary heads. Aspect has a modest correlation with water contents for the entire suction range, unlike the soil attributes. Since aspect is largely independent of soil attributes, it may be a valuable predictor for water contents. The range in aspect values, however, is limited because only one transect was investigated. The three different curvatures do not demonstrate correlation with water contents. The potential radiation in spring and winter, however, are negatively correlated with water contents. Among the soil attributes, only ρ_b and sand show a negative correlation. Since radiation is correlated with neither ρ_b nor sand, spring and winter radiation appear to be useful predictors. The same holds true for $\cos\phi$, with which potential radiation is highly correlated. Lower solar radiation in winter and spring may lead to a more favorable soil structure for water retention.

[28] Third, relations between hydraulic parameters and topography. With the exception of K_s, the correlation was somewhat less as for soil attributes. Tangential curvature has an almost negligible correlation with θ_r. Aspect and radiation indices have respectively a positive and negative correlation with θ_s. The parameters α and n display a negative and a positive correlation with slope and elevation, two correlated topographical attributes. The air entry value will be larger for higher elevations and steeper slopes, whereas the pore-size distribution appears narrower. This may be because soils at higher elevations are less mature while soils with gentle slopes at lower elevations may have a wider range of particle sizes due to weathering, surface runoff and erosion.

[29] The aforementioned topographical correlations are small, but they are in line with the basic soil properties. Soils with greater z and β have a considerably higher organic matter content and also a higher silt fraction, and somewhat lower sand and clay percentages (narrower pore-size distribution). Unlike basic soil properties, K_s did show some correlation with topographical attributes. There was a very slight positive correlation with slope. *Casanova et al.* [2000] also reported such a correlation based on tension infiltrometer measurements; the higher K_s for sloping soils was attributed to less crusting and surface sealing. There was a more pronounced correlation with solar radiation in the spring (and hence fall) as well as the winter. The moisture and thermal regime during these seasons has a strong effect on both water transmission (positive correlation) and retention (negative correlation). Summer radiation does not significantly affect K_s.

[30] The lower correlation of topographical than of soil attributes with hydraulic data is plausible [*Moore et al.*, 1993]. The influence of topography on soil hydraulic properties will be an indirect one, most of the variability that can be explained by topographical attributes can probably be explained by soil attributes as well. Furthermore, there is a difference in spatial resolution and accuracy. Soil attributes were often measured on the same sample used to determine hydraulic properties. On the other hand, the topographical data were obtained from a 30 × 30-m DEM, with elevations at the grid points subject to error, using mathematical operations such as differentiation and interpolation, and errors in location of sampling points. *Thompson et al.* [2001] demonstrated that vertical and horizontal precision greatly affect the accuracy of the estimates for slope and curvature. The absence of correlation for curvature with any of the hydraulic data is probably due to this lack of precision. Compound topographical attributes, such as wetness index or elevation relief ratio, were therefore not evaluated as predictor.

3.2. Neural Network Analysis

[31] Twenty-one ANNs were developed using different combinations of predictors. Table 1 shows the correlation coefficient, r, for regression of predicted and observed hydraulic parameters and RMSE and ME of water contents and log K_s. Also included is the relative difference in RMSE, Δ, between ANNs with and without topographical attributes (given in bold) for identical soil attributes. Adding topographical variables leads to modest improvements in the prediction of most, but not all, retention parameters. It appears that adding elevation, z, could improve RMSE by up to 10% (e.g., model 3 versus 6). If slope, β, is added as well, the improvement will be slight (e.g., model 6 versus 9,

SD		0.062	0.040	0.012	0.25	58	0.04	0.04	0.04	0.05	0.05	0.05	0.05	0.04	0.04	
mean		0.077	0.42	0.0081	1.39	31.3	0.42	0.42	0.40	0.39	0.38	0.37	0.23	0.20	0.18	
unit		---cm^3/cm^3---		cm^{-1}		cm/d	----------cm^3/cm^3----------									
		θ_r	θ_s	α	n	K_s	$\theta_{0.1}$	θ_{10}	θ_{50}	θ_{90}	θ_{150}	θ_{250}	θ_{3b}	θ_{6b}	θ_{12b}	
ρ_b		-0.05	**0.83**	0.17	-0.09	-0.06	**0.83**	**0.79**	**0.65**	**0.59**	**0.58**	**0.56**	0.15	0.19	0.17	ε
ρ_s	**0.30**		-0.04	**-0.49**	**0.66**	-0.18	0.01	0.08	**0.21**	**0.29**	**0.30**	**0.32**	0.05	**0.22**	**0.30**	θ_r
OC	**-0.47**	**-0.36**		0.01	-0.10	-0.14	**1.00**	**0.95**	**0.87**	**0.80**	**0.80**	**0.78**	**0.38**	**0.40**	**0.34**	θ_s
clay	-0.15	-0.08	-0.05		**-0.68**	0.13	-0.01	-0.11	**-0.40**	**-0.48**	**-0.51**	**-0.51**	-0.18	**-0.22**	-0.15	α
silt	**-0.27**	0.10	**0.36**	0.07		-0.08	-0.07	0.02	0.19	**0.27**	**0.26**	**0.26**	**-0.38**	**-0.26**	**-0.26**	n
sand	**0.34**	0.02	**-0.24**	**-0.76**	**-0.65**		-0.17	**-0.20**	-0.18	-0.16	**-0.20**	**-0.20**	-0.13	-0.17	-0.11	K_s
z	**-0.34**	-0.06	**0.62**	-0.05	**0.59**	**-0.37**		**0.96**	**0.87**	**0.80**	**0.80**	**0.79**	**0.37**	**0.38**	**0.33**	$\theta_{0.1}$
β	0.05	-0.15	**0.39**	-0.19	**0.31**	-0.05	**0.44**		**0.89**	**0.83**	**0.84**	**0.82**	**0.37**	**0.40**	**0.34**	θ_{10}
$\cos\phi$	-0.14	0.20	0.09	0.05	0.14	-0.12	**0.21**	-0.17		**0.97**	**0.98**	**0.97**	**0.47**	**0.52**	**0.45**	θ_{50}
PC	-0.01	-0.07	0.03	**-0.28**	0.03	**0.24**	-0.04	0.06	**-0.20**		**0.97**	**0.97**	**0.45**	**0.53**	**0.46**	θ_{90}
TC	0.10	-0.13	0.07	-0.09	-0.05	0.10	-0.00	0.02	**-0.23**	**0.21**		**0.99**	**0.51**	**0.57**	**0.50**	θ_{150}
MC	0.01	-0.16	0.10	**-0.28**	-0.04	**0.26**	-0.01	0.05	**-0.21**	**0.80**	**0.70**		**0.53**	**0.60**	**0.53**	θ_{250}
SpR	0.16	**-0.25**	0.12	-0.17	0.07	0.09	0.09	**0.75**	**-0.65**	**0.25**	0.14	**0.22**		**0.93**	**0.88**	θ_{3b}
SuR	-0.02	0.05	-0.31	**0.24**	**-0.39**	0.03	**-0.47**	**-0.91**	0.09	-0.02	0.03	0.02	**-0.60**		**0.95**	θ_{6b}
WR	0.13	**-0.24**	0.08	-0.17	-0.00	0.13	0.00	**0.63**	**-0.71**	**0.26**	0.14	**0.22**	**0.96**	**-0.47**		
ε	**-0.88**	0.10	**0.31**	0.11	**0.29**	**-0.32**	**0.29**	**-0.12**	0.19	**-0.01**	**-0.16**	-0.07	**-0.26**	0.06	**-0.23**	ε
θ_r	-0.04	-0.07	0.14	**0.25**	0.05	**-0.28**	0.02	0.05	0.15	-0.08	**-0.21**	-0.14	-0.01	0.04	-0.04	θ_r
θ_s	**-0.69**	**0.23**	**0.27**	0.12	**0.44**	**-0.38**	**0.41**	-0.10	**0.28**	0.03	-0.13	-0.05	**-0.29**	0.01	**-0.29**	θ_s
α	-0.18	-0.16	-0.09	**-0.34**	**-0.35**	**0.40**	**-0.21**	**-0.23**	-0.11	0.11	0.03	0.13	-0.07	**0.24**	-0.01	α
n	0.05	0.00	**0.20**	0.15	**0.21**	**-0.23**	**0.23**	**0.29**	0.02	-0.04	-0.13	-0.08	**0.22**	**-0.25**	0.15	n
K_s	0.03	-0.06	0.02	0.01	0.17	-0.17	0.16	**0.22**	-0.18	-0.01	0.01	-0.03	**0.33**	-0.13	**0.31**	K_s
$\theta_{0.1}$	**-0.70**	**0.23**	**0.29**	0.14	**0.45**	**-0.40**	**0.41**	-0.12	**0.29**	0.02	-0.14	-0.06	**-0.31**	0.02	**-0.30**	$\theta_{0.1}$
θ_{10}	**-0.65**	**0.24**	**0.32**	0.19	**0.50**	**-0.46**	**0.44**	-0.05	**0.25**	0.03	-0.16	-0.08	**-0.25**	-0.02	**-0.26**	θ_{10}
θ_{50}	**-0.55**	**0.23**	**0.31**	**0.31**	**0.55**	**-0.55**	**0.48**	0.04	**0.32**	-0.06	-0.14	-0.13	**-0.22**	-0.12	**-0.24**	θ_{50}
θ_{90}	**-0.50**	**0.22**	**0.31**	**0.35**	**0.57**	**-0.59**	**0.45**	0.07	**0.28**	-0.09	-0.16	-0.17	-0.18	-0.16	**-0.20**	θ_{90}
θ_{150}	**-0.46**	**0.27**	**0.26**	**0.37**	**0.54**	**-0.59**	**0.42**	0.03	**0.32**	-0.08	-0.16	-0.17	**-0.22**	-0.11	**-0.25**	θ_{150}
θ_{250}	**-0.45**	**0.27**	**0.24**	**0.40**	**0.52**	**-0.59**	**0.38**	-0.01	**0.33**	-0.10	-0.17	-0.19	**-0.26**	-0.07	**-0.29**	θ_{250}
θ_{3b}	-0.08	**0.21**	-0.09	**0.35**	0.15	**-0.30**	-0.07	**-0.23**	**0.30**	-0.13	-0.05	-0.16	**-0.38**	0.19	**-0.37**	θ_{3b}
θ_{6b}	-0.14	0.16	0.01	**0.45**	0.17	**-0.38**	-0.10	**-0.22**	**0.29**	-0.16	-0.13	**-0.21**	**-0.37**	0.18	**-0.37**	θ_{6b}
θ_{12b}	-0.13	0.11	0.01	**0.44**	0.10	**-0.35**	-0.13	**-0.23**	**0.22**	-0.13	-0.12	-0.19	**-0.32**	**0.24**	**-0.30**	θ_{12b}
	ρ_b	ρ_s	OC	clay	silt	sand	z	β	$\cos\phi$	PC	TC	MC	SpR	SuR	WR	
unit	g/cm^3	g/cm^3	%	%	%	%	m	°		m^{-1}	m^{-1}	m^{-1}	MW/m^2	MW/m^2	MW/m^2	
mean	1.42	2.53	0.20	34.3	40.3	25.4	739	9.67	-0.65	2.2	2.5	2.3	8.48	11.8	4.37	
SD	0.10	0.086	0.17	8.8	7.7	12.0	142	6.14	0.46	22	19	16	5.5	2.2	7.4	

Figure 4. Spearman rank correlations as well as mean and standard deviation of soil, topographical, and hydraulic data. Correlations that are significant ($p < 0.05$) are given in bold.

Table 1. Values of r for Correlation Between Observed and Predicted Hydraulic Parameters, RMSE, Relative Change in RMSE, Δ, by Including Topographical Data and ME of Hydraulic Data Predicted with Neural Network Models for 21 Different Combinations of Predictors[a]

		r					RMSE				ME × 10^3	
ANN	Predictors	θ_r	θ_s	logα	log$n$	logK_s	$\theta(h)$, cm^3/cm^3	Δ $\theta(h)$, %	logK_s	Δ logK_s, %	$\theta(h)$, cm^3/cm^3	logK_s
1	SSC	0.35	0.52	0.62	0.38	0.44	0.039		0.79		−16.1	−3.9
2	SSC, ρ_b	0.38	0.77	0.69	0.40	0.59	0.035		0.73		−9.9	9.3
3	SSC, ρ_b, OC	0.42	0.59	0.62	0.46	0.50	0.036		0.78		−3.1	−14.5
4	SSC, *z*	0.43	0.62	0.66	0.48	0.46	0.037	7.09	0.79	0.51	−9.6	6.9
5	SSC, ρ_b, *z*	0.48	0.79	0.75	0.52	0.59	0.035	1.42	0.74	−1.10	−11.2	−11.4
6	SSC, ρ_b, OC, *z*	0.55	0.81	0.75	0.57	0.64	0.033	8.52	0.71	8.26	−4.2	10.4
7	SSC, *z*, β	0.44	0.69	0.69	0.46	0.48	0.036	8.90	0.78	1.39	−7.9	−10.5
8	SSC, ρ_b, *z*, β	0.48	0.82	0.77	0.54	0.57	0.034	3.70	0.75	−2.48	−8.5	−10.2
9	SSC, ρ_b, OC, *z*, β	0.53	0.82	0.75	0.56	0.56	0.033	10.2	0.76	2.32	−2.0	7.2
10	SSC, *z*, β, **cos**ϕ	0.48	0.71	0.68	0.49	0.59	0.036	9.67	0.74	6.08	−7.6	11.9
11	SSC, ρ_b, *z*, β, **cos**ϕ	0.50	0.81	0.77	0.55	0.57	0.035	−0.85	0.75	−3.58	−10.9	−19.4
12	SSC, ρ_b, OC, *z*, β, **cos**ϕ	0.59	0.83	0.75	0.61	0.60	0.034	6.87	0.74	5.16	−9.1	13.5
13	SSC, *z*, β, ***PC***, ***TC***, ***MC***	0.44	0.68	0.71	0.49	0.49	0.036	9.16	0.78	1.27	−7.3	18.9
14	SSC, ρ_b, *z*, β, ***PC***, ***TC***, ***MC***	0.47	0.81	0.75	0.52	0.56	0.035	0.57	0.75	−3.71	−9.5	34.4
15	SSC, ρ_b, OC, *z*, β, ***PC***, ***TC***, ***MC***	0.54	0.81	0.75	0.58	0.62	0.035	3.30	0.73	5.55	−8.7	26.8
16	SSC, *z*, β, ***SpR***, ***SuR***, ***WR***	0.46	0.71	0.66	0.47	0.60	0.036	9.67	0.73	7.73	−8.7	44.1
17	SSC, ρ_b, *z*, β, ***SpR***, ***SuR***, ***WR***	0.50	0.83	0.77	0.52	0.61	0.033	5.41	0.72	1.24	−8.8	11.3
18	SSC, ρ_b, OC, *z*, β, ***SpR***, ***SuR***, ***WR***	0.52	0.84	0.75	0.56	0.61	0.033	9.07	0.73	6.45	−9.4	14.6
19	*z*, β, **cos**ϕ, ***PC***, ***TC***, ***MC***, ***SpR***, ***SuR***, ***WR***	0.53	0.64	0.53	0.54	0.53	0.040		0.76		−7.0	−38.4
20	SSC, *z*, β, **cos**ϕ, ***PC***, ***TC***, ***MC***, ***SpR***, ***SuR***, ***WR***	0.54	0.72	0.71	0.62	0.59	0.037	6.62	0.74	6.05	−10.3	39.0
21	ρ_b, *z*, β, **cos**ϕ, ***PC***, ***TC***, ***MC***, ***SpR***, ***SuR***, ***WR***	0.53	0.77	0.59	0.58	0.58	0.039		0.742		−8.9	−22.5

[a]Hydraulic data are given in bold.

which happens to produce the most accurate prediction). If aspect, cosϕ, is also used as input variable for the ANN, the prediction becomes worse (models 8 and 9 versus 11 and 12). Solar radiation is somewhat more informative than curvature (models 13–15 versus 16–18), as could already be inferred from the Spearman analysis. Relying solely on topographical data resulted in the worst prediction of retention data (model 19); it is clear that some basic soil properties need to be determined. Using textural data and/or bulk density supplemented with elevation and/or slope as

Table 2. Values of r, RMSE, Relative Change in RMSE, Δ, by Including Topographical Data and ME of Observed Versus Predicted Water Contents at 50 and 12,000 cm as Well as RMSE and ME for Water Contents at 50 and 12,000 cm Described With Equation (1) Using Predictions With Neural Network Models for 21 Different Combinations of Predictors[a]

		Observed							Described With Equation (1)			
		r		RMSE				ME × 10^3		RMSE		ME × 10^3	
ANN	Predictors	θ_{50}	θ_{12b}	θ_{50}, cm^3/cm^3	Δθ_{50}, %	θ_{12b}, cm^3/cm^3	Δ θ_{12b}, %	θ_{50}, cm^3/cm^3	θ_{12b}, cm^3/cm^3	θ_{50}, cm^3/cm^3	θ_{12b}, cm^3/cm^3	θ_{50}, cm^3/cm^3	θ_{12b}, cm^3/cm^3
1	SSC	0.66	0.55	0.032		0.033		−0.8	0.1	0.033	0.043	−4.7	−25.6
2	SSC, ρ_b	0.78	0.54	0.027		0.034		−0.3	0	0.028	0.044	3.9	−23.8
3	SSC, ρ_b, OC	0.69	0.56	0.031		0.033		−0.1	−0.4	0.033	0.040	9.1	−18.1
4	SSC, *z*	0.73	0.59	0.030	8.64	0.033	2.69	−1.3	1.0	0.031	0.042	3.9	−23.4
5	SSC, ρ_b, *z*	0.81	0.57	0.026	4.80	0.033	2.07	0.4	0	0.027	0.045	3.7	−27.8
6	SSC, ρ_b, OC, *z*	0.89	0.61	0.026	18.2	0.032	4.20	−0.6	−0.4	0.029	0.039	7.8	−16.1
7	SSC, *z*, β	0.77	0.59	0.028	13.6	0.033	2.69	−0.9	0.6	0.030	0.042	5.1	−21.5
8	SSC, ρ_b, *z*, β	0.82	0.57	0.025	6.64	0.033	2.07	−0.2	0.3	0.027	0.042	4.2	−21.2
9	SSC, ρ_b, OC, *z*, β	0.83	0.60	0.025	21.7	0.032	3.00	−0.6	0.2	0.028	0.039	9.5	−14.8
10	SSC, *z*, β, **cos**ϕ	0.81	0.61	0.026	19.8	0.032	4.49	−0.5	−0.1	0.030	0.042	6.5	−22.4
11	SSC, ρ_b, *z*, β, **cos**ϕ	0.83	0.60	0.025	8.12	0.032	4.44	−0.5	0.5	0.027	0.046	5.0	−28.4
12	SSC, ρ_b, OC, *z*, β, **cos**ϕ	0.84	0.63	0.024	23.0	0.032	4.80	−1.0	−1.1	0.027	0.042	3.9	−20.8
13	SSC, *z*, β, ***PC***, ***TC***, ***MC***	0.76	0.59	0.028	13.0	0.033	2.40	0.1	−0.5	0.031	0.041	5.9	−20.3
14	SSC, ρ_b, *z*, β, ***PC***, ***TC***, ***MC***	0.82	0.59	0.026	5.17	0.033	3.25	−0.8	−0.1	0.028	0.043	4.7	−23.8
15	SSC, ρ_b, OC, *z*, β, ***PC***, ***TC***, ***MC***	0.82	0.61	0.026	18.5	0.032	3.90	0.2	1.0	0.029	0.043	5.3	−23.1
16	SSC, *z*, β, ***SpR***, ***SuR***, ***WR***	0.81	0.64	0.026	20.4	0.031	6.89	−0.6	−0.3	0.030	0.043	5.9	−24.2
17	SSC, ρ_b, *z*, β, ***SpR***, ***SuR***, ***WR***	0.83	0.63	0.024	9.96	0.032	6.21	−0.3	1.1	0.027	0.042	5.4	−23.4
18	SSC, ρ_b, OC, *z*, β, ***SpR***, ***SuR***, ***WR***	0.85	0.66	0.023	26.2	0.031	8.41	−1.4	−1.0	0.027	0.042	4.5	−23.3
19	*z*, β, **cos**ϕ, ***PC***, ***TC***, ***MC***, ***SpR***, ***SuR***, ***WR***	0.66	0.45	0.034		0.036		0.1	1.3	0.036	0.043	7.2	−21.3
20	SSC, *z*, β, **cos**ϕ, ***PC***, ***TC***, ***MC***, ***SpR***, ***SuR***, ***WR***	0.81	0.65	0.026	20.4	0.031	7.19	−0.1	0.3	0.031	0.044	4.6	−25.6
21	ρ_b, *z*, β, **cos**ϕ, ***PC***, ***TC***, ***MC***, ***SpR***, ***SuR***, ***WR***	0.72	0.49	0.031		0.036		1.3	0.4	0.033	0.044	5.7	−23.3

[a]Hydraulic data are given in bold.

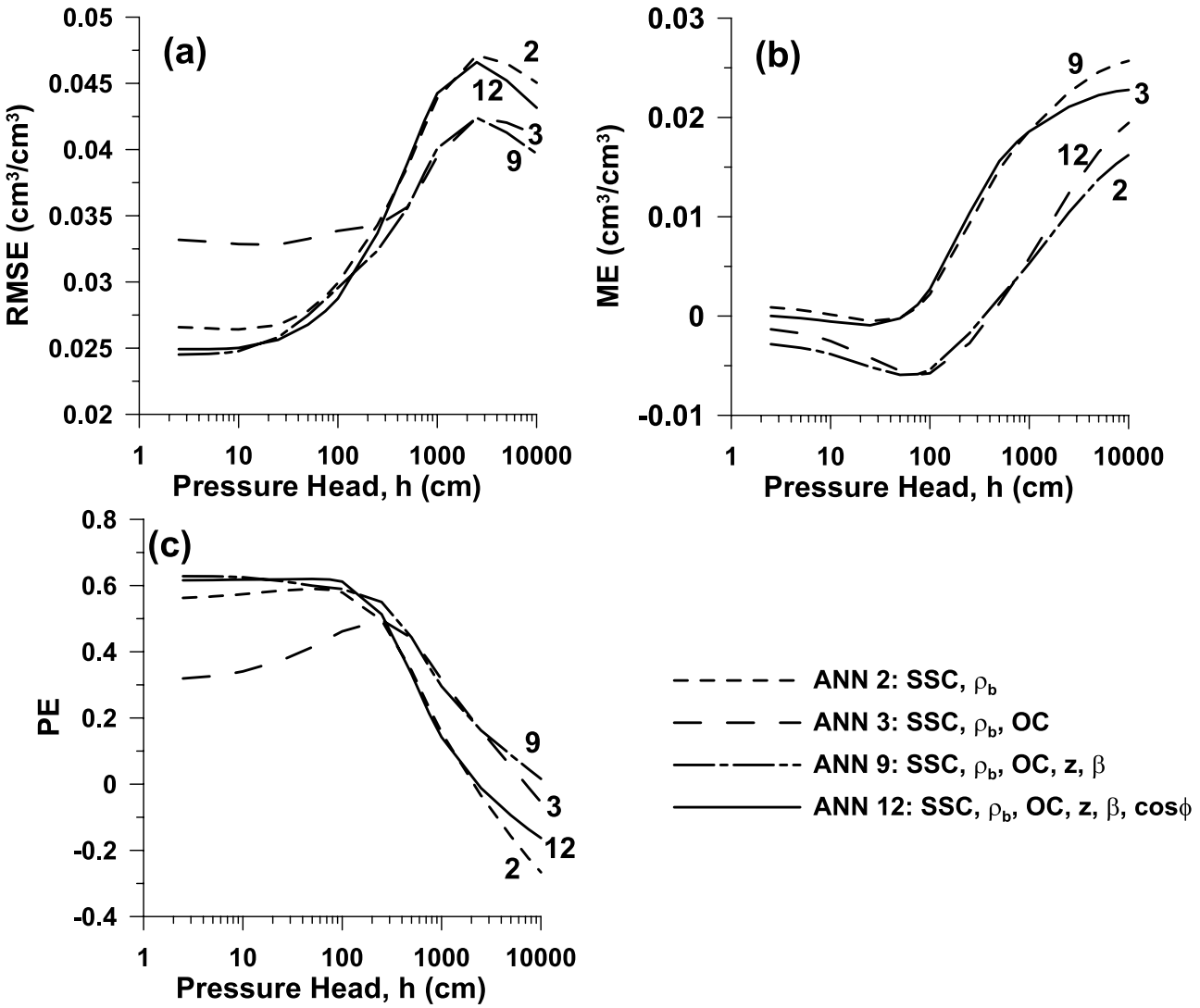

Figure 5. RMSE, MSE and PE as a function of h for ANNs 2, 3, 9, and 12.

predictors appears to be the best strategy. If more topographical predictors are included, the neural network models become excessively parameterized (e.g., model 4 versus 20). The organic carbon content has no predictive value in the absence of topographical variables (model 2 versus 3). If elevation or elevation and slope are used as predictor, including organic carbon yields more accurate estimates (models 5 versus 6 and 8 versus 9). Apparently, the type of organic carbon is more informative than the quantity.

[32] Turning to the saturated hydraulic conductivity, the RMSE values confirm the findings of Figure 4 that topographical data tend to provide marginally improved predictions. Model 6, with texture, bulk density, organic carbon and elevation as input, yields the most accurate prediction based on RMSE. The results confirm that, at least for our data set, solar radiation is a better predictor than land surface curvature. Solar radiation affects the spatial variation of both water content and soil temperature. The latter will be especially pronounced during wetter periods and impact chemical and biological processes. The ME values in Table 1 suggest that the neural network models systematically underpredict the retention data $\theta(h)$ as described by equation (1).

[33] Sometimes the prediction of specific water contents is of interest. Table 2 shows statistical results for the prediction of water contents at 50 cm and 12 bar, the ANNs were trained on observed water contents for, again, 21 different sets of predictors. For "wet" conditions (θ_{50}), including topographical variables led to greater improvements of RMSE than was found for hydraulic parameters in Table 1. For example, including z and β may decrease RMSE by more than 20% (model 3 versus 9). The improvements for dry conditions (i.e., θ_{12b}) are modest. This is in line with the findings by *Western et al.* [1999] for surface water content in a catchment area near Melbourne, Australia. On the other hand, *Famiglietti et al.* [1998] reported that the influence of topography on surface water content for a hillslope in Austin, Texas is more pronounced during "dry" conditions. This could be due to correlations between topography and clay content. Model 18, with elevation, slope, and solar radiation as topographical attributes, provides the most accurate predictions for both wet and dry conditions. As comparison, results are also included for prediction of hydraulic parameters with ANNs (see Table 1) and subsequent calculation of θ_{50} and θ_{12b} with equation (1).

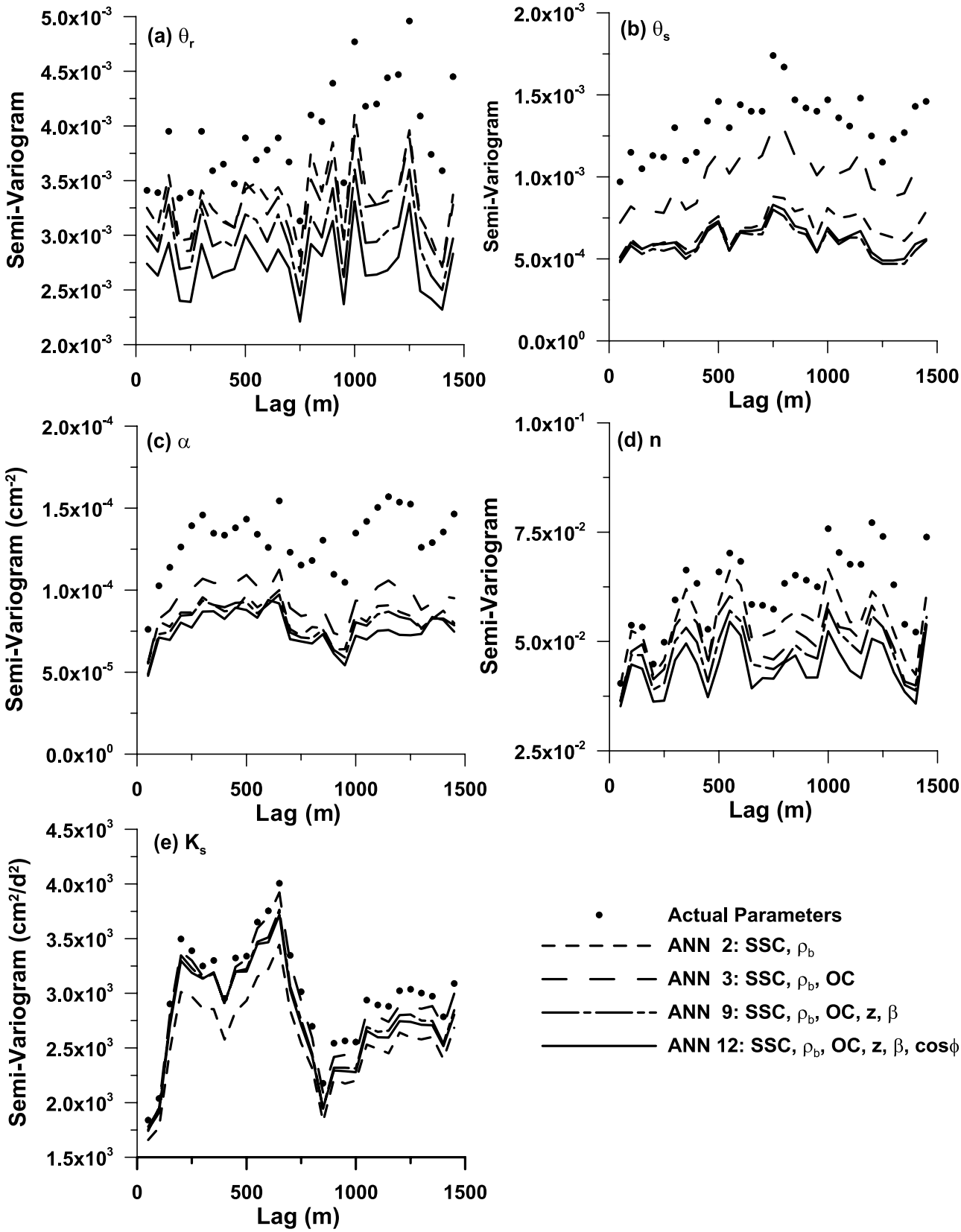

Figure 6. Semivariogram of θ_r, θ_s, α, n, and K_s and their residuals (i.e., difference between observations and predictions with ANNs 2, 3, 9, and 12).

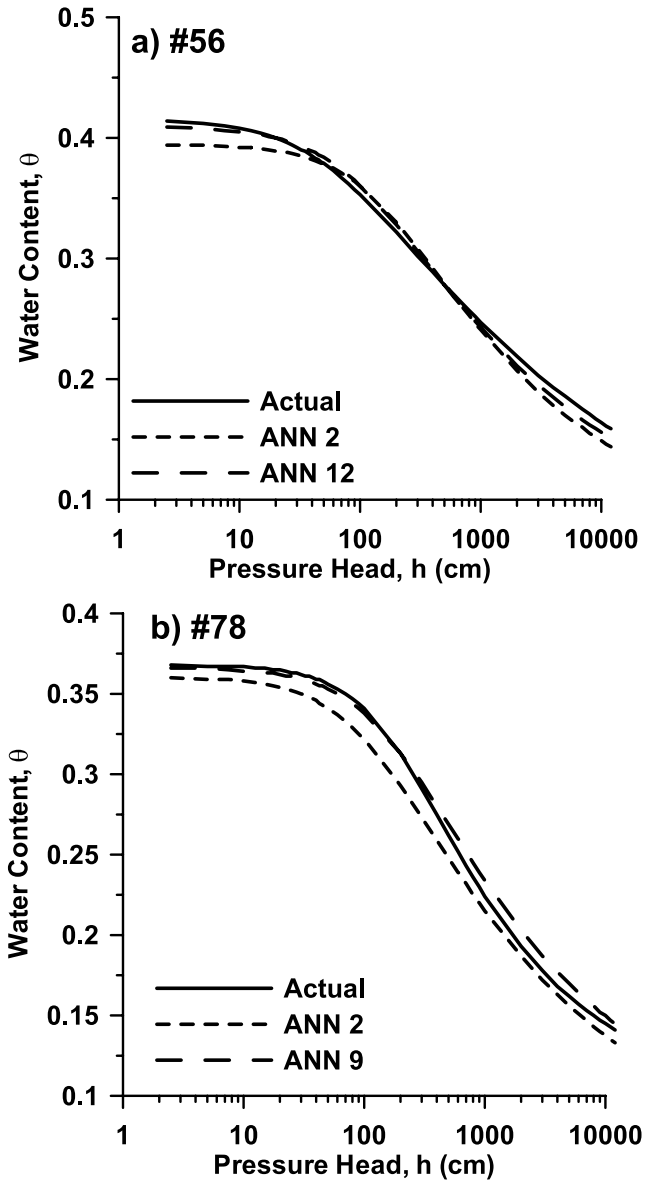

Figure 7. Observed and predicted retention curves for positions 56 and 78.

Not surprisingly, the prediction with these ANNs is less accurate than for the case where the ANN was trained on direct observations, especially for the water content at 12 bar. *Minasny and McBratney* [2002] suggested calibrating the ANNs for the prediction of hydraulic parameters using an objective function of observed and fitted water contents.

[34] The behavior of the ANNs with soil moisture regime was investigated by examining predictions as a function of capillary head, h. Figure 5a shows values for the RMSE for models 2, 3, 9, and 12 as a function of h. The predictions are more accurate for wetter conditions ($h < 100$ cm). The simplest model 2 performs actually better than model 3 for the higher saturations, including organic matter only pays off for $h > 250$ cm. Model 9 provides the most accurate predictions. Adding elevation and slope to the predictors of model 3 results in considerably better predictions in the wet range, but has virtually no impact for drier conditions where organic carbon already appears to be a useful predictor. If aspect is also added as predictor, the performance of the ANN deteriorates to that of the simplest case (models 2 versus 12).

[35] Systematic underpredictions or overpredictions may be detected with the value of ME. Figure 5b illustrates the ME(h) curves for the four ANNs. Models 2 and 12 exhibit little systematic bias below $h = 100$ cm, but they greatly overpredict water content for drier conditions. In general, models 3 and 9 have less systematic prediction errors except that they do underestimate water content near saturation. The increase in ME in the dry range may be caused by a lack of sampling points and because the employed predictors are more meaningful for capillary bound water at lower h. Including aspect helps the prediction at lower but not at higher h.

[36] Figure 5c shows the prediction index (PE) given by equation (9) as a function of soil water pressure head. Model 3 provides the least efficient prediction, most noticeably in the wet range ($h < 250$ cm). Model 9 appears to be the most efficient predictor, but even this ANN yields inferior estimates for very dry conditions ($h > 10$ bar).

[37] Figures 6a–6e contain the semivariograms of "observed" θ_r, θ_s, α, n, and K_s, respectively. Furthermore, each plot contains semivariograms of residuals ($\Delta = f - \hat{f}$) using the predictions made with ANNs 2, 3, 9, and 12. The semivariogram of the hydraulic parameters and the residuals quantify the total variability and the unexplained variability, respectively. The greater the difference between them, the better the predictions by the ANN. Figure 6a displays the erratic behavior of θ_r, increasing the number of predictors leads to more accurate ANNs although a considerable amount of variability is unexplained. On the other hand, θ_s can be explained more accurately as shown in Figure 6b. Model 3 performs relatively poor. Interestingly, the other models are able to explain most of the spatial variability; the semivariograms of the residuals are relatively flat compared to that of the observed θ_s. The same holds true for α, although including organic carbon without any topographical data (model 3) is not quite as bad as for θ_s. Figure 6d demonstrates that the ANNs are not very successful to predict n (see Table 1), but that including more predictors does improve the predictions. As noted before, prediction of K_s is problematic for this data set and the ANN with the simplest predictors (model 2) provides the best results. On the basis of the semivariograms, it appears that topographical attributes are particularly useful to predict θ_r and n, and to explain spatial variability in θ_s and α. Periodograms were also computed; these will not be shown because most of the variability ("power") of both parameters and residuals was associated with frequencies <0.01 cycles/point. Sampling at closer intervals is required to obtain more informative

Table 3. Predicted and Observed Retention Parameters for Locations 56 and 78

Location	ANN	θ_r	θ_s	α, cm^{-1}	n
56	observed	0	0.42	0.017	1.18
56	2	0.063	0.39	0.007	1.32
56	12	0.051	0.41	0.010	1.27
78	observed	0.096	0.37	0.005	1.43
78	2	0.055	0.36	0.009	1.29
78	9	0.065	0.37	0.006	1.31

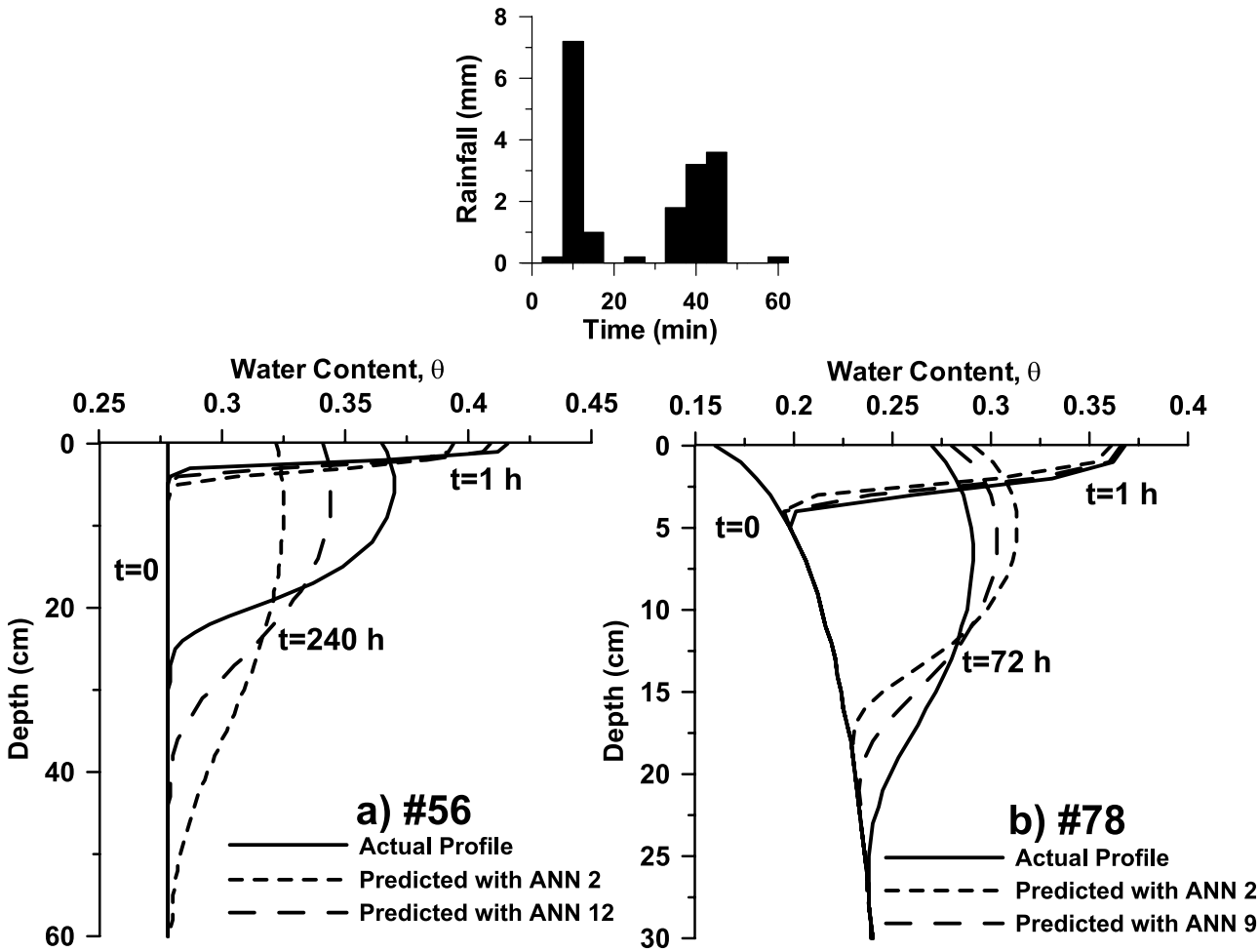

Figure 8. Water content profiles during infiltration and redistribution for positions 56 and 78.

periodograms. The semivariograms and the analysis by *Santini et al.* [1999] suggest the presence of different soil-landscape units ranging from 400 to 800 m.

3.3. Application

[38] Observed retention data and predicted curves for a few illustrative ANNs are shown in Figure 7 for locations 56 (z = 746 m, $\beta = 3.12°$) and 78 (z = 636 m, $\beta = 8.37°$). Table 3 lists the observed and predicted retention parameters. In both cases, the retention curve is predicted with model 2 using texture, i.e., percentages sand, silt and clay (SSC), and bulk density as predictor. For #56, the curve was also predicted with model 11. The addition of organic carbon, elevation, slope, and aspect as predict appears to improve the prediction over the whole range of water contents. For location 78 aspect was omitted in the second ANN (i.e., model 9), topographical variables and OC improved the prediction of retention perhaps with the exception of the dry range.

[39] The observed and predicted retention parameters were used as input to the program HYDRUS [*Šimůnek et al.*, 1998] to simulate water movement in the upper soil profile at locations 56 and 78 during and after rainfall, no attempt was made to account for hysteresis or root extraction. The water flux at the soil surface was specified to resemble a high intensity rain shower followed by an evaporation of 0.005 cm/h. The unsaturated hydraulic conductivity was described according to *Mualem* [1976] using a pore-connectivity parameter of -1 [*Schaap and Leij*, 2000]. Because saturated conductivity was poorly predicted, we used the measured K_s of 0.019 and 0.009 cm/h for locations 56 and 78, respectively. Figure 8a shows water content profiles for site 56 after 1 hour (at the end of the infiltration stage) and after 240 hours (redistribution stage) using three sets of retention parameters and a uniform initial water content. The insert in Figure 8a shows the rainfall distribution as observed during a 1-hour period on 16 August 1997. The "actual" wetting front is steeper and penetrates less far than the fronts predicted with ANNs 2 and 12. The discrepancy is greatest for ANN 2, which has no topographical predictors. The likely reason is that the ANNs underpredict $\theta_s - \theta_r$ and α compared to the observed parameters. Similar profiles are shown in Figure 8b for location 78 for a nonuniform initial water content using ANNs 2 and 9. In this case the "true" wetting front penetrates faster and the water content changes less abruptly than predicted with ANNs 2 and 9. The likely reason is that the ANNs predict a higher $\theta_s - \theta_r$ and lower n. Again, the greatest difference occurs for the ANN with no topographical predictors.

4. Summary and Conclusions

[40] Unsaturated hydraulic and other soil properties were determined at 50-m intervals along a 5-km hillslope as part

of a study regarding the hydrology, surface erosion, and land degradation of the Sauro river catchment area in Basilicata, Southern Italy. Several studies have shown that hydraulic properties, especially surface water content, might be correlated with topographical attributes. The present work was undertaken to quantify if hydraulic parameters could be predicted more accurately when topographical attributes were included as predictors in PTFs.

[41] Analysis of Spearman rank correlations revealed that the retention parameters are somewhat correlated with z, β, $\cos\phi$ and potential solar radiation. A fairly strong correlation was found between z and OC and silt fraction while an inverse relation was found with ρ_b and sand fraction. Correlations between retention and topographical parameters tend to be smaller than those between the former and basic soil properties and retention parameters. Virtually no correlation was found between retention parameters and curvature of the land surface, presumably due to errors involved in the determination of curvature. The data set did not reveal correlation between K_s and soil properties, but K_s was correlated with β and potential radiation in spring (fall) and winter. Correlation was also investigated for observed water contents. In the wet range (low h), topography was more strongly correlated with water content than retention parameters.

[42] Twenty-one ANNs were developed to predict retention parameters, K_s, and water contents at h = 50 cm and 12 bar. The prediction of retention parameters could be improved by 10% by including topography. The most accurate prediction was obtained (RMSE = 0.0327 cm^3 cm^{-3}) with ANN 9, which used textural fractions, ρ_b, OC, z, and β as predictors. Furthermore OC became a better predictor when the PTF also includes z, with which it is highly correlated. The water content at h = 50 cm could be predicted 26% more accurately (RMSE = 0.0231 $cm^3 cm^{-3}$ for ANN 18 with texture, ρ_b, OC, z, β, and potential solar radiation as input), but improvement for K_s was modest. The predictions of ANNs were further investigated by plotting RMSE, ME, and PE as a function of h. Predictions with and without topographical attributes were most accurate in the wet range. Semivariograms of the hydraulic parameters and their residuals for ANNs 2, 3, 9 and 12 showed that the ANN could explain some of the (spatial) variability, especially for θ_s and, to a smaller extent, α and n.

[43] The data of this study suggest that including topographical attributes as predictors for PTFs may lead to improvements in the prediction of hydraulic parameters. On the basis of the semivariograms, including topographical variables is most useful for the poorly predictable θ_r and n, and to predict spatial variability in θ_s and α. The implications of differently predicted retention curves were demonstrated with simulated water content profiles. The small influence of topography on predictions, as already reported in some earlier studies, is not surprising because most "information" from topography will already be included in the basic soil properties and there may be considerable uncertainty associated with topographical attributes.

[44] An even more promising use of topographical variables involves the prediction of either soil or hydraulic parameters when limited or no basic soil properties are available. Such a scenario will be common for study of the vadose zone over larger scales such as catchments. Given the empiricism of neural networks and the use of only one transect to calibrate them, the results of this study can not readily be applied for predictions at other locations where conditions may be different. However, this study should provide the impetus for further use of topographical attributes as predictors for hydraulic data.

[45] **Acknowledgments.** The experimental work for this study was conducted under the direction of Prof. Alessandro Santini as part of research project MIUR-PRIN2000 entitled "Impiego di modelli di simulazione nella gestione dell'irrigazione." This project also partly funded the stay of the first author in Italy. Funding by the NSF (EAR-9876800) through SAHRA at the University of Arizona partly supported research in the United States.

References

Ahuja, L. R., D. K. Cassel, R. R. Bruce, and B. B. Barnes (1989), Evaluation of spatial distribution of hydraulic conductivity using effective porosity data, *Soil Sci.*, *148*, 404–411.

Bouma, J. (1989), Using soil survey data for quantitative land evaluation, *Adv. Soil Sci.*, *9*, 177–213.

Carter, B. J., and E. J. Ciolkosz (1991), Slope gradient and aspect effects on soil development from sandstone in Pennsylvania, *Geoderma*, *49*, 199–213.

Casanova, M., I. Messing, and A. Joel (2000), Influence of aspect and slope gradient on hydraulic conductivity measured by tension infiltrometer, *Hydrol. Processes*, *14*, 155–164.

Cerdà, A. (1997), Seasonal changes of infiltration rates in a Mediterranean scrubland on limestone, *J. Hydrol.*, *198*, 209–225.

Cosby, B. J., G. M. Hornberger, R. B. Clapp, and T. R. Ginn (1984), A statistical exploration of the relationships of soil moisture characteristics to the physical properties of soils, *Water Resour. Res.*, *20*, 682–690.

Dane, J. H., and G. C. Topp (Eds.) (2002), *Methods of Soil Analysis*, part 4, *Physical Methods*, Soil Sci. Soc. of Am., Madison, Wis.

Demuth, H., and M. Beale (1992), Neural network toolbox manual, MathWorks, Inc., Natick, Mass.

Famiglietti, J. S., J. W. Rudnicki, and M. Rodell (1998), Variability in surface moisture content along a hillslope transect: Rattlesnake Hill, Texas, *J. Hydrol.*, *210*, 259–281.

Goovaerts, P. (1997), *Geostatistics for Natural Resources Evaluation*, Oxford Univ. Press.

Gupta, S. C., and W. E. Larson (1979), Estimating soil water retention characteristics from particle size distribution, organic matter percent, and bulk density, *Water Resour. Res.*, *15*, 1633–1635.

Hanna, Y. A., P. W. Harlan, and D. T. Lewis (1982), Soil available water as influenced by landscape position and aspect, *Agron. J.*, *74*, 999–1004.

Hawley, M. E., T. J. Jackson, and R. H. McCuen (1983), Surface soil moisture variation on small agricultural watersheds, *J. Hydrol.*, *62*, 179–200.

Heuvelink, G. B. M., and E. J. Pebesma (1999), Spatial aggregation and soil process modeling, *Geoderma*, *89*, 47–65.

Merz, B., and E. J. Plate (1997), An analysis of the effects of spatial variability of soil and soil moisture on runoff, *Water Resour. Res.*, *33*, 2909–2922.

Minasny, B., and A. B. McBratney (2002), The *neuro-m* method for fitting neural network parametric pedotransfer functions, *Soil Sci. Soc. Am. J.*, *66*, 352–361.

Minasny, B., A. B. McBratney, and K. L. Bristow (1999), Comparison of different approaches to the development of pedotransfer functions for water-retention curves, *Geoderma*, *93*, 225–253.

Mitášová, H., and J. Hofierka (1993), Interpolation by regularized spline with tension: II Application to terrain modeling and surface geometry analysis, *Math. Geol.*, *25*, 657–669.

Moore, I. D., G. J. Burch, and D. H. Mackenzie (1988), Topographic effects on the distribution of surface water and the location of ephemeral gullies, *Trans. ASAE*, *31*, 1098–1107.

Moore, I. D., P. E. Gessler, G. A. Nielsen, and G. A. Peterson (1993), Soil attribute prediction using terrain analysis, *Soil Sci. Soc. Am. J.*, *57*, 443–452.

Mualem, Y. (1976), A new model predicting the hydraulic conductivity of unsaturated porous media, *Water Resour. Res.*, *12*, 513–522.

Pachepsky, Y. A., D. Timlin, and W. J. Rawls (2001), Soil water retention as related to topographic variables, *Soil Sci. Soc. Am. J.*, *65*, 1787–1795.

Press, W. H., B. P. Flannery, S. A. Teukolsky, and W. T. Vetterling (1988), *Numerical Recipes in C*, Cambridge Univ. Press, New York.

Rawls, W. J., and D. L. Brakensiek (1989), Estimation of soil water retention and hydraulic processes, in *Unsaturated Flow in Hydrologic Modeling: Theory and Practice*, *NATOASISer., Ser. C*, vol. 9, edited by H. J. Morel-Seytoux, pp. 275–300, Kluwer, Norwell, Mass.

Rawls, W. J., D. L. Brakensiek, and K. E. Saxton (1982), Estimation of soil water properties, *Trans. ASAE*, *25*, 1316–1320.

Romano, N., and A. Santini (1997), Effectiveness of using pedo-transfer functions to quantify the spatial variability of soil water retention characteristics, *J. Hydrol.*, *202*, 137–157.

Romano, N., J. W. Hopmans, and J. H. Dane (2002), Water retention and storage: Suction table, in *Methods of Soil Analysis*, part 4, *Physical Methods*, edited by J. H. Dane and G. C. Topp, pp. 692–698, Soil Sci. Soc. of Am., Madison, Wis.

Ruhe, R. V. (1956), Geomorphic surfaces and the nature of soils, *Soil Sci.*, *82*, 441–455.

Ruhe, R. V. (1975), *Geomorphology*, Houghton Mifflin, Boston, Mass.

Santini, A., A. Coppola, N. Romano, and F. Terribile (1999), Interpretation of the spatial variability of soil hydraulic properties using a land system analysis, in *Modelling of Transport Processes in Soils*, edited by J. Feyen and K. Wiyo, pp. 491–500, Wageningen Acad., Wageningen, Netherlands.

Schaap, M. G., and F. J. Leij (1998), Database-related accuracy and uncertainty of pedotransfer functions, *Soil Sci.*, *163*, 765–779.

Schaap, M. G., and F. J. Leij (2000), Improved prediction of unsaturated hydraulic conductivity with the Mualem-van Genuchten model, *Soil Sci. Soc. Am. J.*, *64*, 843–851.

Schaap, M. G., F. J. Leij, and M. T. van Genuchten (2001), Rosetta: A computer program for estimating soil hydraulic parameters with hierarchical pedotranfer functions, *J. Hydrol.*, *251*, 163–176.

Shumway, R. H., and D. S. Stoffer (2000), *Time Series Analysis and Its Applications*, Springer-Verlag, New York.

Šimůnek, J., K. Huang, M. Sejna, and M. T. van Genuchten (1998), The HYDRUS-1D software package for simulating the one-dimensional movement of water, heat, and multiple solutes in variably-saturated media, version 1.0, *IGWMC- TPS - 70*, Int. Ground Water Model. Cent., Colo. Sch. of Mines, Golden.

Sinowsky, W., A. C. Scheinost, and K. Auerswald (1997), Regionalisation of soil water retention curves in a highly variable soilscape. II. Comparison of regionalisation procedures using a pedotransfer function, *Geoderma*, *78*, 145–159.

Thompson, J. A., J. C. Bell, and C. A. Butler (2001), Digital elevation model resolution: Effects on terrain attribute calculation and quantitative soil-landscape modeling, *Geoderma*, *100*, 67–89.

U.S. Army Corps of Engineers (1993), GRASS4.1 reference manual, Construction Eng. Res. Lab., Champaign, Ill.

van Genuchten, M. T. (1980), A closed form equation for predicting the hydraulic conductivity of unsaturated soils, *Soil Sci. Soc. Am. J.*, *44*, 892–898.

Vereecken, H., J. Maes, J. Feyen, and P. Darius (1989), Estimating the soil moisture retention characteristic from texture, bulk density, and carbon content, *Soil Sci.*, *148*, 389–403.

Walker, P. H., F. F. Hall, and R. Protz (1968), Relation between landform parameters and soil properties, *Soil Sci. Soc. Am. Proc.*, *32*, 101–104.

Western, A. W., R. B. Grayson, G. Blöschl, G. R. Willgoose, and T. A. McMahon (1999), Observed spatial organization of soil moisture and its relation to terrain indices, *Water Resour. Res.*, *35*, 797–810.

Western, A. W., G. Blöschl, and R. B. Grayson (2001), Towards capturing hydrologically significant connectivity in spatial patterns, *Water Resour. Res.*, *37*, 83–97.

Wösten, J. H. M., Y. A. Pachepsky, and W. J. Rawls (2001), Pedotransfer function: Bridging the gap between available basic soil data and missing soil hydraulic characteristics, *J. Hydrol.*, *251*, 123–150.

Yaalon, D. H. (1997), Soils in the Mediterranean region: What makes them different?, *Catena*, *28*, 157–169.

A. Coppola, Department DITEC, University of Basilicata, C.da Macchia Romana, 85100 Potenza, Italy.

F. J. Leij and M. G. Schaap, GEBJ Salinity Laboratory, 450 W. Big Springs Road, Riverside, CA 92507, USA.

M. Palladino and N. Romano, Department of Agricultural Engineering, Division for Land and Water Resources Management, University of Naples "Federico II", Via Università, 100, 80055 Portici (NA), Italy. (nunzio.romano@unina.it)